



ELSEVIER

Available online at www.sciencedirect.com

SCIENCE @ DIRECT®

Nuclear Instruments and Methods in Physics Research A 538 (2005) 408–415

NUCLEAR
INSTRUMENTS
& METHODS
IN PHYSICS
RESEARCH
Section A

www.elsevier.com/locate/nima

Comparison of a silicon photomultiplier to a traditional vacuum photomultiplier[☆]

V.D. Kovaltchouk^a, G.J. Lolos^{a,*}, Z. Papandreou^a, K. Wolbaum^b

^a*Department of Physics, University of Regina, Regina, SK, Canada, S4S 0A2*

^b*Faculty of Science, University of Regina, Regina, SK, Canada, S4S 0A2*

Received 21 June 2004; received in revised form 16 August 2004; accepted 24 August 2004

Available online 19 October 2004

Abstract

Silicon photomultiplier devices (SiPM) were investigated as a possible front-end detector system for the electromagnetic barrel calorimeter of the GlueX Project at Jefferson Laboratory, USA, and compared against a traditional 2 in vacuum photomultiplier tube. The SiPM has gain and timing resolution comparable to that of a PMT, requires a simple electronic circuit and is not sensitive to magnetic fields. These attributes allow us to conclude that it is feasible to use the SiPM as a front-end detector for this calorimeter.

© 2004 Elsevier B.V. All rights reserved.

PACS: 29.40.Gx; 29.40.Mc; 42.81.Cn; 85.60.Dw

Keywords: Silicon photomultiplier; Scintillating fiber; Barrel calorimeter

1. Introduction

The goal of the GlueX/Hall D experiment [1–3] at Jefferson Laboratory in Newport News (Virginia, USA) is to search for gluonic excitations manifested in exotic hybrid vector mesons with masses up to $2.5 \text{ GeV}/c^2$ using linearly polarized

photons of 8–10 GeV energy. The decay products of the produced mesons must be identified and measured with good resolution and with full acceptance for all decay angles. As such, the GlueX detector system must have the capability of measuring the emission angles and energies of neutral particles and the four-momenta of charged particles with good overall resolution to allow for a complete kinematic reconstruction of events and subsequent partial wave analysis [3].

The electromagnetic barrel calorimeter (BCAL) is a crucial GlueX/Hall D detector subsystem. BCAL will be positioned immediately inside the

[☆]This paper reports on research carried out on behalf of the GlueX/Hall D collaboration at Jefferson Lab in Newport News, VA USA

*Corresponding author. Tel.: +1 306 585 4248; fax: +1 306 585 5659.

E-mail address: george.lolos@uregina.ca (G.J. Lolos).

super-conducting solenoid, which constrains its outer radius to be 90 cm, and will be approximately 4 m long and 25 cm thick. The calorimeter will be constructed using at least 4 m long scintillating fibers (SciFi), 1 mm in diameter, embedded in a lead matrix of successive layers of lead (0.5 mm thick) and SciFis. The readout system has to collect the scintillation light—with peak emission in the range 350–500 nm—from about 3.2 m² of active surface of the barrel calorimeter. As a result, the front-end detector and the readout system must achieve an energy resolution as good or better than 5%/√*E*(GeV) [4], and adequate timing resolution. For example, the requirement of 10 cm spatial resolution translates into a timing resolution of $\sigma = 150$ ps for a Gaussian fit. The anticipated count rate of events is about 10⁶ events/s within the magnetic field created by the superconducting solenoid with a central value greater than 2 T.

Traditional vacuum photomultiplier tubes (PMT), hybrid photo-diodes (HPD) and silicon photomultipliers (SiPM) have been investigated [5] as possible front-end detectors, whereas the HPD and the PMT have proven unsuitable, the most promising results were obtained with the SiPM.

2. Silicon photomultiplier

Although single-pixel Geiger mode devices (Avalanche Photo Diodes—APDs) were developed in the mid sixties, the SiPM is a novel type of APD [6]. It is a promising device for our application in GlueX, since it is insensitive to magnetic fields, has a high gain ($\sim 10^6$), good quantum efficiency, provides excellent timing resolution (~ 120 ps for single photo-electron detection) and a fast risetime (sub-ns), achieves good dynamic range ($\sim 10^3$ /mm²), and does not suffer from nuclear counter effects when operated in Geiger mode. Finally, it has a solid performance at room temperature (in contrast to VLPCs) and does not exhibit any serious radiation damage effects, other than perhaps from neutrons [7].

The SiPM is a multi-pixel photo-diode with a large number of micro-pixels (500–1500 each with a typical size of 20–30 μ m) joined together on a

common substrate and under a common load. The photodiode has a multi-layer structure with different doping levels. As a result, within the thin depletion region between p⁺ and n⁺ layers, a very high electric field of about 5×10^5 V/cm is created, with the right conditions for a Geiger discharge mode to take place.

The operational bias voltage is 10–20% higher than breakdown voltage, with typical supplied bias voltage of 50–60 V. The diode is reverse biased to increase the field in the depletion region.

The pixels are electrically decoupled from each other and operate in a Geiger mode, limited by the charge accumulated in the pixel capacitor. The Geiger discharge ceases when the voltage drops to values below the breakdown value due to the external resistor on each pixel. Each pixel detects and amplifies the charge from a photon, independently of all other pixels, and its signal does not depend on the impinging number of quanta that fire the pixel in a Geiger mode. The total number of pixels defines the dynamic range of the photodetector.

The gain for a single pixel is determined by the accumulated charge in the capacitor of the pixel (typically $C_{\text{pixel}} = 100$ pF) and depends on an over-voltage: $Q = C_{\text{pixel}}(V_{\text{bias}} - V_{\text{breakdown}})$, where V_{bias} and $V_{\text{breakdown}}$ are the supplied bias and breakdown voltages, respectively. Due to its high gain, the electronics noise of the SiPM is negligibly small and the main source of the noise is the dark rate.

The single pixel gain is approximately 10⁶, roughly the same order of magnitude as that of a traditional PMT. While each pixel operates digitally as a binary device—because all SiPM pixels work together on a common load and there is a large number of pixels—the output signal is a sum of the signals from all pixels registering a “hit”. Thus, the SiPM, as whole, is an analogue detector that can measure the incident light intensity. The distribution of the voltage across the depletion depth of 4–6 μ m is such that for only a fraction of the depth (~ 1 –2 μ m) the former exceeds a value sufficient for Geiger discharge creation, and therefore, the Geiger discharge is contained within this limited region. As a result, its duration is very short, a few hundreds of ps, resulting in typical rise times of 1 ns.

The SiPMs photon detection efficiency, η , is given by $\eta = QE\varepsilon$, where η is the photon detection efficiency, QE is the quantum efficiency and ε is a geometrical factor. The latter is a ratio of the sensitive area (as defined by the total active pixel area) to the total area. This value does not depend on wavelength and is a constant for each SiPM. The devices used in our particular tests had geometrical factors of 0.3/1.0 for all SiPMs/PMTs investigated, respectively. The quantum efficiency is a function of incident wavelength of light and has a maximum in the 500–600 nm region, decreasing monotonically for lower wavelengths. The efficiency, η , for the SiPMs is about 20% for $\lambda = 550$ nm, a value considerably larger than that of a 2" Burle 8575 PMT at this wavelength (5%). However, for $\lambda = 400$ nm, the SiPM has a lower value of η than a PMT, and as a result is more sensitive in the green–yellow region of wavelength than the PMT, an attribute that has practical implications since scintillators exist for the UV–blue and green–yellow spectrum.

The SiPMs used in our tests were developed and produced by the Moscow Engineering and Physics Institute (MEPHI) in cooperation with a state enterprise (PULSAR). The specific SiPMs had 1000 pixels in each detector covering the 1 mm² sensitive area and the supplied bias voltage was 50–60 V. Although the geometrical factor for these SiPMs was 0.3, efforts are underway at MEPHI/PULSAR to increase this to as much as 0.7. Competitors at the University of Obninsk in cooperation with a private firm (CPTA) [8] claim that their device has 50% higher photon detection efficiency in the green region and fewer constraints on mechanical performance. Moreover, the Obninsk/CPTA team is carrying out R&D towards the manufacturing of 3 × 3 mm² SiPM active area wafers and is also investigating the construction of larger areas by connecting SiPMs in a matrix configuration [8].

3. Tests with a nitrogen plasma discharge tube

The purpose of this work was to investigate SiPMs as front-end detectors for the barrel calorimeter readout system, as defined by the

requirements of the GlueX/Hall D Project. Specifically the SiPMs were investigated under the following two conditions:

- Detection of incident light of high flux intensity, where about 200–500 SiPM pixels registered a hit, but the signal was not saturated.
- Detection of light of lower photon flux intensity in which case only few pixels registered a hit. This regime corresponds to a few-photon-counting condition.

3.1. High photon flux tests

An Optitron nanosecond broad spectrum optical pulse radiator (Model NR-1A) with a Nitrogen Plasma Discharge Tube¹ was used as a source of light for the SiPM investigation under high photon flux conditions. The light pulses had a 1 ns rise time and a few ns pulse duration, and were measured with the SiPM as well as with a 2" Burle PMT (model 8575). A clear, pure fused silica fiber of 5 m length was used to transport the light from the Optitron plasma discharge tube to the sensitive surface of the SiPM. The light intensity emitted from this tube could be varied within a broad range of amplitudes and was monitored by the PMT.

Pulses from the SiPM and the PMT were measured with a Tektronix TDS-5104 digital oscilloscope, as shown in Fig. 1. The supplied high voltage to the PMT was 1900 V while the bias for the SiPM was 55.5 V. The signals from the SiPM and PMT were each split in two, with one branch fed to an ADC (LeCroy 2249A) and the other to a Constant Fraction Discriminator (CFD Tennelec TC455) whose output was then fed to a TDC (LeCroy 2228A). In this measurement, the trigger signal from the plasma discharge unit acted as the “start” signal for the TDC unit.

The detected signal amplitude for the SiPM was ~300 mV, corresponding to ~200–300 pixels registering a hit. This performance rendered the use of an external amplifier unnecessarily. More-

¹Optitron Inc. 23206 Normandie Ave. #8, Torrance, CA 90502, USA.

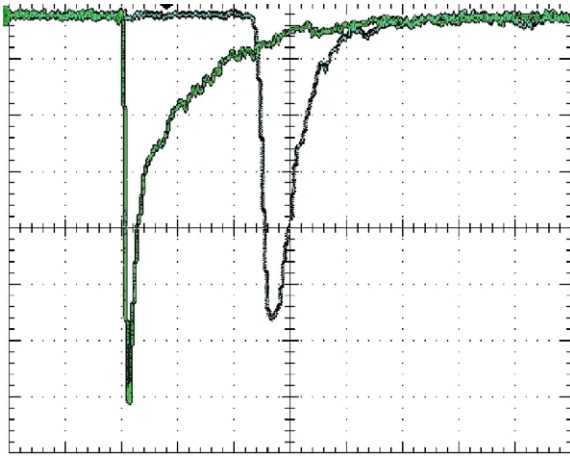


Fig. 1. The shape of pulses from SiPM (left) and PMT (right). A light flasher (Optitron Inc.) was used as a light source. The horizontal and vertical scales are 20 ns/div and 100 mV/div, respectively.

over, the signal from the SiPM exhibited no saturation as was concluded from the linear dependence of its ADC amplitude versus light intensity. Whereas the timing distributions have a similar structure with risetimes of 1 and 4 ns for the SiPM and PMT, respectively, the former has a σ that is less than half of the latter's: $\sigma = 140$ ps vs. 375 ps.

3.2. Low photon flux tests

In order to investigate the energy resolution of the SiPM, we measured the pulse amplitude distribution under low photon flux conditions employing the Optitron unit and a neutral-density attenuation filter that reduced the light to 1% of its initial value.

The amplitude of the signals in the SiPM, in this case, was 5–10 mV, and this necessitated the use of a fast amplifier (LeCroy 612A). Under such conditions it was not possible to eliminate completely the noise pick-up from electronic equipment present in the area, especially the noise originating from the plasma discharge unit. While RF (pick-up) noise was present in all measurements that utilized the plasma discharge unit, this noise was negligible under high photon flux conditions. However, when only a few pixels

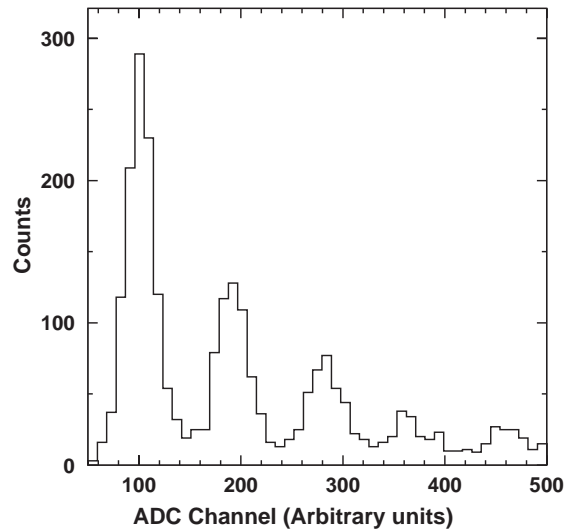


Fig. 2. SiPM pulse height spectrum for low-intensity light pulses.

generate output, even low amplitude noise contributes to the overall resolution. Nevertheless, the pulse amplitude distribution shown in Fig. 2 exhibits five well-separated peaks corresponding to single photon detection and good separation for emission of up to five photoelectrons. The 2" Burle 8575 PMT cannot resolve individual photoelectron peaks.

4. SiPM as a front-end detector for a 4-m scintillating fiber

Next, we evaluated the performance of the SiPM used as a front-end detector for light signals produced by minimum ionization particles traversing a 4-m-long Kuraray SCSF-81 single-clad SciFi. Fibers with similar parameters will be used in the barrel calorimeter for GlueX/Hall D detector system. The schematic diagram of the experimental setup is shown in Fig. 3.

Kuraray SCSF-81 SciFi's have an emission spectrum range of 400–550 nm, peaking at 437 nm, with a 2.4 ns scintillation decay time and an attenuation length of ~ 3.5 m. The fiber had a 1 mm outer diameter and the cladding thickness was 3% of the diameter. One end of the fiber was

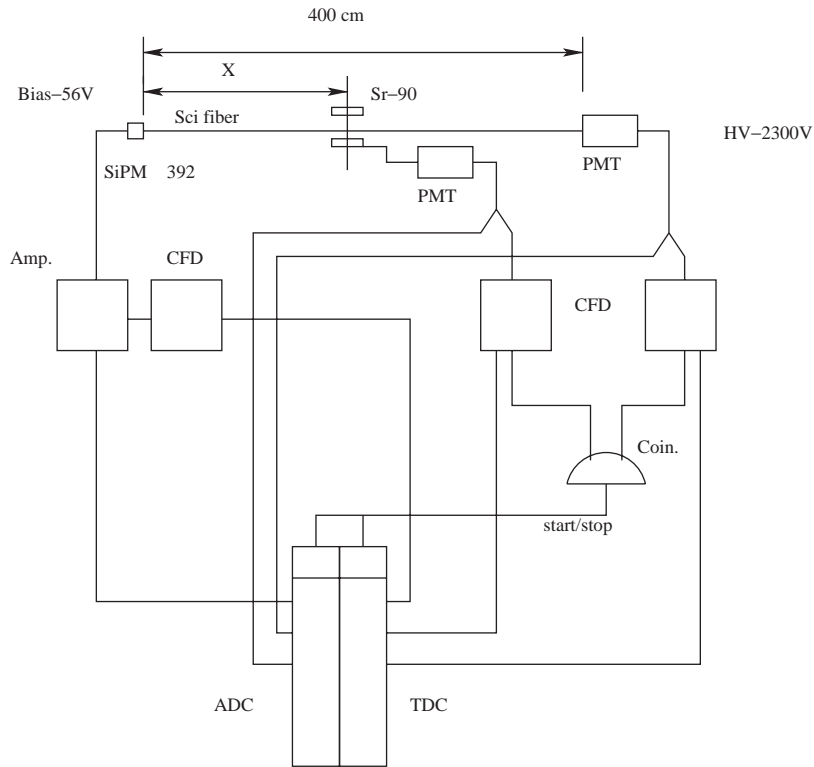


Fig. 3. The electronics diagram of the experimental setup using a 4-m scintillating fiber coupled to a SiPM and PMT.

connected to the SiPM and the other to the PMT. Both ends of the SciFi were polished to increase the light transmission and a special arrangement was used to preserve the optical connection between the fiber and the sensitive surfaces of the PMT and the SiPM. The fiber was in direct contact with the surface of the PMT window, while it had a 0.3–0.5 mm air gap between the end of the fiber and the sensitive surface of the SiPM in order to prevent damage to the SiPM. It should be noted that the Burle 8575 PMT has a 25% efficiency at the peak of the Kuraray emission wavelength while the SiPMs efficiency for that region is about 15%. As a result, for the same light intensity from the scintillating fiber, the SiPM exhibits a photon detection efficiency that is 60% of the PMTs. The comparison in efficiency between the two devices is summarized in Table 1.

The scintillating fiber was excited using a ^{90}Sr (^{90}Y) beta source with 2280 keV maximal and 935 keV average energy of beta particles. The

ionization source had 0.1 μCi activity. The difference in the distributions of ionization energy loss in the scintillating-fiber core, as calculated by a Monte-Carlo simulation for the triggering beta particles and compared to the minimum ionization particles, is only a few percent on average [9].

An aluminum collimator for beta particles was used to improve the signal-to-noise ratio. The distance between the ionization source and the fiber was 0.5 cm. A “trigger” detector was placed under the fiber and the ionization source and it registered the beta particles passing through the scintillating fiber. The signals from the PMTs were split into two paths. One, after a delay, was directed to an ADC for amplitude spectrum measurement. The second path passed through a constant fraction discriminator (Ortec CFD 455) set to minimize the “walk” correction of the signals from the PMTs. The coincidence (LeCroy 465) between the two PMTs signals created a “start” signal for the Camac ADC/TDC units.

Table 1
Detection efficiency, $\eta = QE\varepsilon$, for the SiPMs and PMTs

| λ (nm) | Device | ε | QE (%) | η (%) |
|----------------|--------|---------------|--------|------------|
| 550 | SiPM | 0.3 | 60 | 20 |
| | PMT | 1.0 | 5 | 5 |
| 437 | SiPM | 0.3 | 45 | 15 |
| | PMT | 1.0 | 25 | 25 |

The integration time window for the TDC unit was set to 120 ns.

The signal from the SiPM was amplified by a fast 12-channel amplifier (LeCroy 612A) that has a 200 MHz bandwidth, fast rise time, DC-coupling, 1 mV stability at the output, 0.1% integral linearity and insures a faithful reproduction of signal shape after amplification. The gain factor was set to 10. One output pulse of the amplifier was digitized by a ADC 2249A unit. The second was put through a CFD en route to a TDC unit.

The TDC and ADC spectra were accumulated and analyzed to extract the dependence of the detected light and timing resolution as a function of distance of the source from the respective readout end of the fiber. The mean values of the distributions were used in the calculation of the attenuation length and are plotted in Fig. 4.

The experimental data were fit with an exponential curve, $y = I \cdot \exp(-x/L)$, where I is the amount of light produced at the interaction point, L is the attenuation length and x is the distance to the ionization source. The ratios of the mean values for the two identical positions of an ionization source are larger for the PMT in comparison with the SiPM. As a result, two different attenuation lengths were obtained for the same fiber, $L_{\text{SiPM}} = 251$ cm and $L_{\text{PMT}} = 146$ cm for the SiPM and the PMT data, respectively, stemming from the difference in the spectral sensitivity of these two devices. The SiPM is more sensitive to longer values of λ where the transmission loss for the Kuraray fiber is lower. Therefore, the SiPM “realizes” a longer attenuation length compared to the PMT. Obviously, the SiPM-fiber combination provides a clear advantage over the PMT-fiber one, in applications where long fibers must be used.

The TDC peak location (the mean value of the Gaussian fit) was plotted versus the distance from the front-end detector and is displayed in Fig. 5. The slopes of the linear fits for the SiPM and the PMT agree with each other within the error of measurement, and are equal to 1.32 ± 0.01 and 1.33 ± 0.01 ch/cm for the SiPM and the PMT experimental data, respectively. The TDC conversion factor was 47 ps/ch. The calculation of the velocity of light propagation gives $v = (1.60 \pm 0.03) \times 10^8$ m/s, a value that agrees with the Kuraray SciFi specifications sheet.

The timing resolution is an important factor in the determination of the position of a particle traversing the fiber, and is presented in Fig. 6 as a function of the distance of the ionization source from each front-end detector. The start signal was provided by the coincidence unit between the trigger detector and the front end PMT. The data presented in Fig. 6 have not been corrected for the time jitter of the trigger detector. Additionally, the quoted timing resolution for the SiPM combines the intrinsic SiPM resolution plus the jitter connected with the LeCroy 612 amplifier.

The smallest values of sigma were 1.5 and 1.1 ns for the SiPM and the PMT, respectively, corresponding to the minimal distance between the ionization source and the front-end detector. The resolution increases/decreases monotonically as the ionization source moves away/towards the front-end detector.

Finally, the timing resolution depends on the number of detected photoelectrons. The average number of photoelectrons detected for the closest position of the ionization source from each front-end detector was ~ 3 –5 for the SiPM and ~ 5 –8 for the PMT. The resultant timing resolutions for the SiPM and for the PMT were comparable.

5. Conclusions

The properties of a SiPM working in Geiger-limited mode have been measured and compared with a standard 2" vacuum PMT. The measurement with the nitrogen plasma discharge unit shows that the SiPM can achieve better time and energy resolutions under high photon flux. To

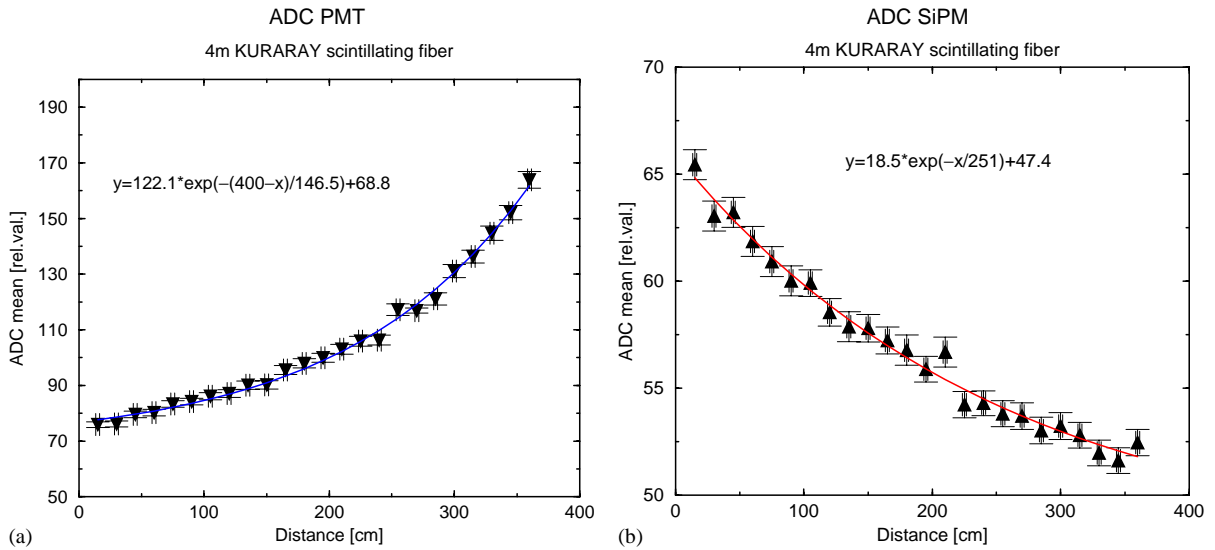


Fig. 4. The dependence of the scintillating light yield with distance from the SiPM is shown for the PMT (left) and the SiPM (right).

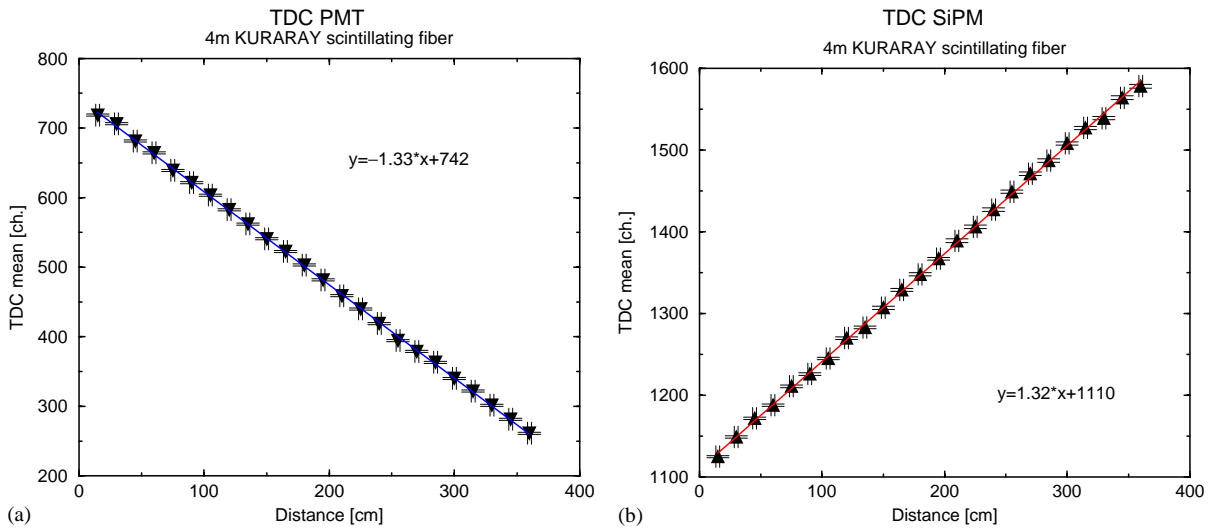


Fig. 5. The time propagation of the scintillating light along the fiber. The left (right) graph corresponds to the PMT (SiPM) experimental data.

evaluate the possibility of using the SiPM as a front-end detector for an electromagnetic calorimeter readout system, we measured the ADC/TDC spectra from the SiPM for 4m scintillating fiber irradiated by ^{90}Sr beta source. Coupled to the performance attributes of SiPMs, the results of

these investigations demonstrated that SiPMs satisfy the basic requirements for such an application. The only outstanding issue that remains is the determination of the coupling choice between the calorimeter's scintillating fibers and the SiPMs, something that may be accomplished with the use

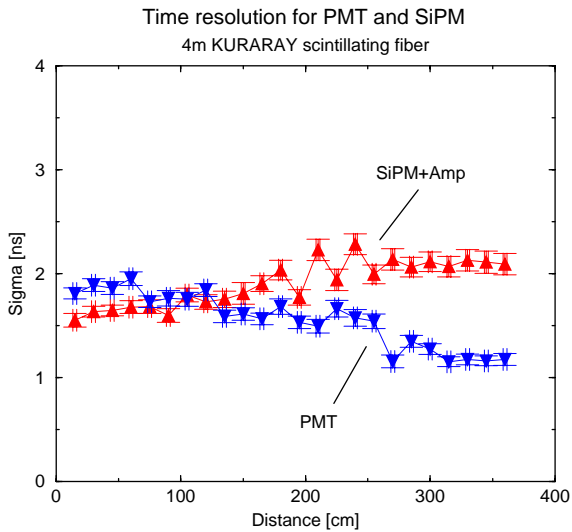


Fig. 6. The timing resolution as a function of the distance from the SiPM detector.

of intermediate wavelength shifter fibers, as attempted for the TESLA experiment [10].

Acknowledgements

This experiment was supported in part by NSERC (Canada) and Jefferson Lab (USA). The

Southeastern University Research Association (SURA) operates the Thomas Jefferson National Accelerator Facility for the US Department of Energy under contract DE-AC05-84ER40150.

References

- [1] GlueX/Hall D Collaboration, The Science of Quark Confinement and Gluonic Excitations, GlueX/Hall D Design Report, Ver. 4, 2002, <http://www.phys.cmu.edu/halld>.
- [2] A.R. Dzierba, C.A. Meyer, E.S. Swanson, Am. Sci. 88 (2000) 406.
- [3] G.J. Lolos, Eur. Phys. J. A 17 (2002) 499.
- [4] M. Adinolfi, KLOE Collaboration, et al., Nucl. Instr. and Meth. A 494 (2002) 326.
- [5] V.D. Kovaltchouk, et al., Hall D Notes 52 and 69, http://www.phys.cmu.edu/halld/notes_main.html.
- [6] B. Dolgoshein, et al., Nucl. Instr. and Meth. A 504 (2003) 48.
- [7] D. Renker, talk presented at the Vienna Conference on Instrumentation, February 16–21, 2004, <http://vci.oew.ac.at/>.
- [8] V. Saliev, talk presented at DESY FLC, March 2004.
- [9] T. Okusawa, et al., Nucl. Instr. and Meth. A 459 (2001) 440.
- [10] B. Dolgoshein, Talk presented at the Vienna Conference on Instrumentation, February 16–21, 2004, <http://vci.oew.ac.at/>.